

# Design and fabrication of indium phosphide air-bridge waveguides with MEMS functionality

Wing H. Ng<sup>\*a</sup>, Nina Podoliak<sup>b</sup>, Peter Horak<sup>b</sup>, Jiang Wu<sup>a</sup>, Huiyun Liu<sup>a</sup>, William J. Stewart<sup>b</sup>, and Anthony J. Kenyon<sup>a</sup>

<sup>a</sup>Department of Electronic and Electrical Engineering, University College London, Torrington Place, London WC1E 7JE, UK

<sup>b</sup>Optoelectronics Research Centre, University of Southampton, Highfield, Southampton SO17 1BJ, UK

## ABSTRACT

We present the design and fabrication of a dual air-bridge waveguide structure integrated with MEMS functionality. The structure is designed to function as a tunable optical buffer for telecommunication application.

The optical buffer structure is based on two parallel waveguides made of high refractive index material with sub-wavelength dimensions. They are suspended in air, and are separated by a sub-micron air gap. Due to the fact that the size of the waveguides is much smaller than the wavelength of light that propagates in the structure, a significant fraction of the optical mode is in the air gap between the waveguides. By changing the size of the air gap using MEMS techniques, we can vary this fraction and hence the effective refractive index of the waveguide structure, thus generating tunable optical delay.

The optical buffer structure was grown on an InP substrate by molecular beam epitaxy, and the device layer was made of InGaP. An InGaAs layer was sandwiched between the device layer and the substrate to serve as a sacrificial layer. The sub-micron waveguides, their supports in the form of side pillars with tapered shapes in order to minimize optical losses, and the MEMS structures were patterned using electron beam lithography and plasma etching. Electrodes were integrated into the structure to provide electrostatic actuation. After the sample patterning, the waveguide structure was released using HF etch. Our simulations predict that by varying the waveguide separation from 50 nm to 500 nm, we could achieve a change in propagation delay by a factor of two.

**Keywords:** Optical buffer, waveguide, III-V semiconductors, MEMS, MOEMS, optical delay, actuation.

## 1. INTRODUCTION

Micro-electromechanical systems (MEMS) are embedded in our everyday life and their applications are immensely diverse, from accelerometers [1] in our mobile phones to bio-MEMS devices for bio-sensing [2-4]. Most of the MEMS structures in semiconductors are manufactured in silicon materials. This is due to the fact that micro- and nano-fabrication of silicon material are well established and widely used, such that silicon-based technology covering a wide range of devices is available at low cost. By contrast, MEMS in other types of semiconductors such as III-V-based materials are not common. In this paper, we demonstrate the design and fabrication of an InP-based dual air-bridge waveguide structure with side pillar supports and incorporated MEMS functionality. The device is designed to function as an optical buffer [5], and the MEMS actuation is designed to provide tunability of the optical delay generated in the buffer. For this particular application, using InP offers significant advantages over silicon. This is because InP is a direct bandgap material, and optical gain can be achieved on-chip or even within the MEMS device itself to compensate for optical losses.

[\\*w.ng@ucl.ac.uk](mailto:w.ng@ucl.ac.uk); phone +44 207-679-2162; [www.ee.ucl.ac.uk](http://www.ee.ucl.ac.uk)

## 2. WAVEGUIDES AND SUPPORTING PILLARS DESIGN

The InP coupled waveguide structure is designed to function as a continuously tunable optical buffer at telecom wavelengths around 1550 nm [5]. The structure consists of two parallel waveguides suspended in air and separated by an air gap. In order for the waveguides to provide the required functionality, a waveguide dimension of 200 nm by 300 nm was found to give the largest group index contrast by varying the air gap. Due to the fact that the waveguide and gap dimensions are much smaller than the wavelength of light propagating through the structure, the optical mode is confined in both waveguides rather than in a single individual waveguide, and also a significant fraction of the optical mode is in the air around the waveguides. Figure 1 shows the simulation of the optical mode (symmetric TE superposition mode) profile for air gaps of 50 nm and 500 nm. It should be noticed that at these air gap and waveguide dimensions, the system supports only the symmetric modes, shown in Figure 1, while the antisymmetric modes are below cut-off [6]. Changing the size of the air gap effectively changes the mode confinement in the waveguides and hence the mode refractive index. As a result, the group propagation delay of a propagating light pulse can be varied in our dual waveguide system.

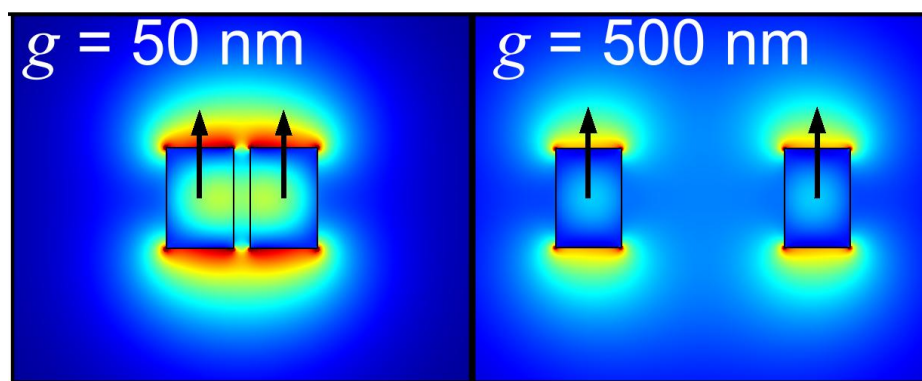


Figure 1. Optical TE mode profile for 50nm and 500nm air gap between coupled InP waveguides of dimensions 200 nm × 300 nm calculated at 1550 nm wavelength.

In order to keep the optical loss due to coupling to bottom substrate or any nearby material negligible, the waveguides should be fully suspended in air at a distance  $>3 \mu\text{m}$  above the bottom substrate and away from any side walls. Waveguides are designed to be supported by pillars connected from the side (T-type connections), which however could cause significant scattering and leakage of light at the connection point (see Figure 2(a)). To minimize these losses at the pillar intersections, two geometries of pillar connections were investigated: multimode interference (MMI)-type connections and S-shaped connections (geometries of which are shown in Figure 2(b) and (c)). The optimal dimensions of the connections which minimize losses were found by modelling light propagation through a section of the waveguide with one pillar (using the finite element method in COMSOL Multiphysics®).

The T-connection at a pillar junction introduces optical loss of more than 1 dB per pillar. Moreover, it also causes a phase delay between two waveguides, disrupting the symmetric propagating mode. The MMI-connection of the optimal dimensions of 1  $\mu\text{m}$  half-width and 5.9  $\mu\text{m}$  length would reduce the losses down to 0.2 dB at an air gap of 200 nm. However, the loss at the MMI-connection is air gap dependent, as the effective index of the optical mode entering the MMI structure changes with varying the gap. The optical loss calculated for the MMI-connection with an air gap of 500 nm becomes 0.5 dB. For the S-shaped connection of dimensions  $0.5 \times 8 \mu\text{m}$ , the loss is less than 0.2 dB and independent of the air gap throughout the 100 to 500 nm air gap variation. Moreover, unlike the MMI-connection, the S-connection operation principle is based on adiabatic mode conversion, thus the loss in this case is not sensitive to small variations in the connection size as induced for example by manufacturing uncertainties.

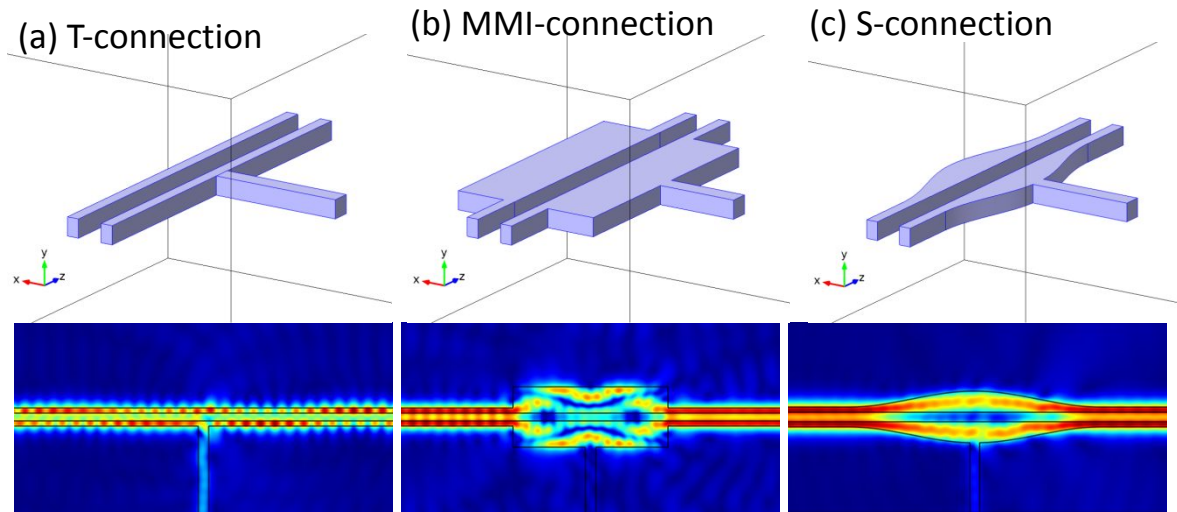


Figure 2. Geometries of pillar connection to the waveguide and the corresponding electric field amplitude of TE-like propagating mode (top view).

### 3. MEMS ACTUATION SCHEME

The tunability of the optical buffer relies on changing the separation between the waveguides. This can be achieved by using electrostatic actuation. In our proposed actuation scheme, voltage of the same polarity is applied to the two waveguides, and the bottom substrate ( $\sim 3 \mu\text{m}$  below the waveguides) is grounded. The electrostatic repulsion causes the initially closely spaced waveguides to be pulled apart.

Figure 3 shows a schematic geometry of the waveguide structure with and without MEMS actuation. The waveguides are parallel and straight when no voltage is applied. When the voltage is applied to the structure, the waveguides are bent under electrostatic repulsion. The staggered position of the supporting pillars causes the waveguides to form a periodic shape, and this ensures minimal variation in the waveguide separation along the device length upon actuation.

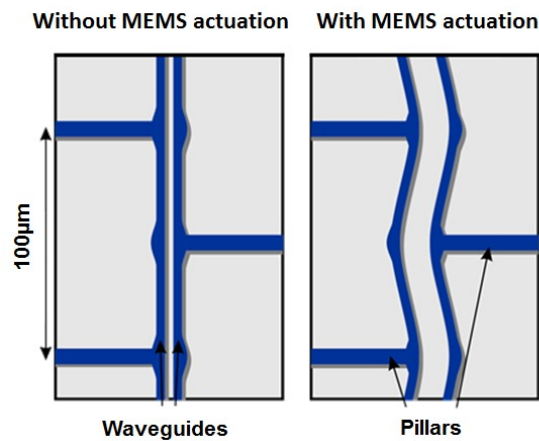


Figure 3. Schematic diagram of the waveguides configurations with and without voltage applied (not to scale).

In order to apply a voltage directly to the waveguides, the waveguide material needs to be doped. This leads to an increase in optical loss due to free-carrier absorption. However, we estimated that for a doping concentration of  $5 \times 10^{17} \text{ cm}^{-3}$ , the free-carrier absorption loss is 2.5 dB/cm, which is comparable to the expected loss due to waveguide surface roughness.

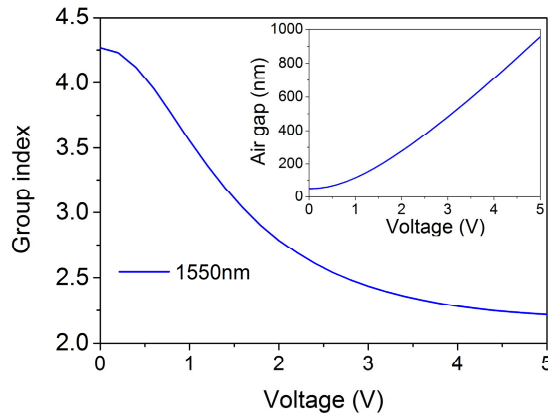


Figure 4. Group index change of the TE mode vs applied voltage at 1550 nm. The inset shows the amount of waveguide separation generated as a function of applied voltage. An initial waveguide separation of 50 nm is assumed.

Using numerical simulations, we modelled waveguide bending in the proposed actuation scheme. The inset of Figure 4 shows the average waveguide separation calculated for a range of voltages applied between the waveguides and the bottom substrate. Knowing the separation between the waveguides, we can then calculate the average group index of the propagating TE mode depending on the applied voltage (Figure 4, main picture). The waveguide separation at 0 Volts is assumed to be 50 nm. We estimate that 4 V is required to separate the waveguides by ~600 nm, and this would give a group refractive index change of ~90% at 1550 nm.

#### 4. FABRICATION

The InP MEMS device was fabricated on an InP substrate with a  $4 \mu\text{m}$   $\text{In}_{0.53}\text{Ga}_{0.47}\text{As}$  layer and a  $300 \text{ nm}$  n-doped InGaP layer (doping concentration  $5 \times 10^{17} \text{ cm}^{-3}$ ) grown by molecular beam epitaxy. The sample structure is shown in Figure 5. A small fraction of 1% of Ga was incorporated in the InGaP layer to give the structure a slight tensile stress in order to prevent the waveguides from collapsing after the waveguide release step in the fabrication process (see below).

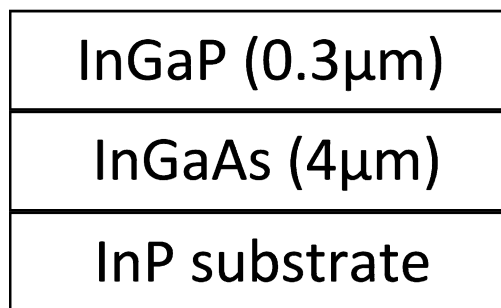


Figure 5. Schematic diagram of the MBE grown structure for InP waveguides with MEMS.

The waveguide fabrication started with patterning the electrode area on the InGaP layer with electron beam lithography (Raith 150-TWO) followed by deposition of a 100 nm Cr/Au layer by thermal evaporation, and lift-off with acetone. The dual waveguides and pillar supports were patterned again with electron beam lithography and using hydrogen silsesquioxane as a negative mask. After the waveguide patterning, the structure was dry etched (by reactive ion etching, RIE) using a cyclic methane-hydrogen/oxygen plasma. Figure 6 shows an SEM image of a waveguide and pillar section taken from a 45° angle. It shows that the reactive ion etch was very anisotropic with side wall angle better than 80°, and also the area between the waveguides was fully etched. The etch depth was measured to be 400 nm, sufficiently large to ensure that the InGaP layer was completely etched through.

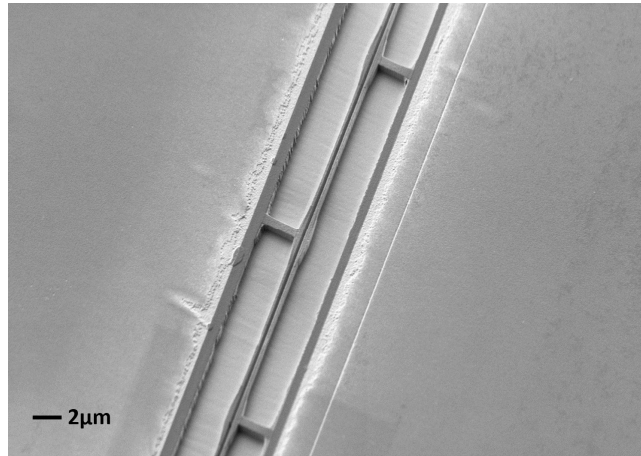


Figure 6. SEM image of the reactive ion etched waveguide and pillar structure. The etch was very anisotropic and the side wall profile is better than 80 degrees.

The waveguide release step was performed after the RIE, and it consisted of two parts – etching of the InGaAs sacrificial layer and supercritical drying. The InGaAs etching was performed using hydrofluoric acid  $\text{HF}:\text{H}_2\text{O}_2:\text{H}_2\text{O}$  (1:1:8) solution. This step etched away the InGaAs layer cleanly without leaving any residue on the waveguide surface. The etched structure was then transferred to a supercritical dryer where the structure was dried using supercritical  $\text{CO}_2$ . A section of the suspended waveguide structure is shown in Figure 7. The cross-sectional dimension of the waveguides was 200 nm by 300 nm and the total length of the waveguides was 200  $\mu\text{m}$ . In our initial structure, the spacing between the pillar supports was set to be 40  $\mu\text{m}$  rather than 100  $\mu\text{m}$  as envisaged in our design. This allowed an increase of the number of pillar sections in our structure to check the consistency of the fabrication.

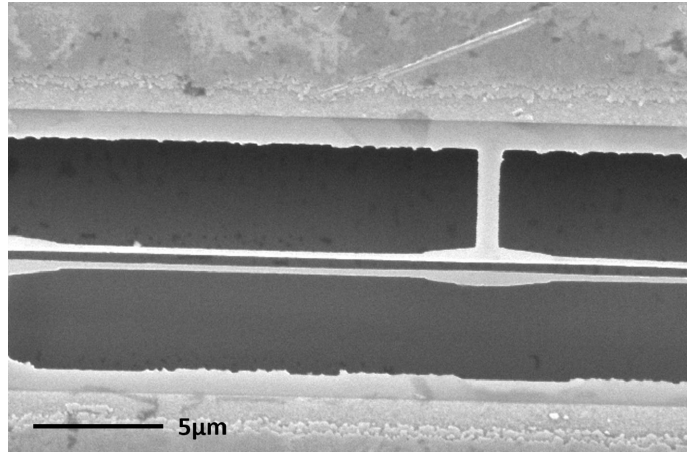


Figure 7. SEM image of a section of the released dual InP air-bridge waveguides suspended in air. The air gap between the waveguides is clearly visible.

## 5. CONCLUSION

We have discussed the design and successfully demonstrated the fabrication of an InP based air-bridge dual waveguide structure with incorporated MEMS functionality. The structure was designed to be used as an optical buffer. The MEMS actuation was designed to adjust the spacing between the initially closely spaced waveguides and it was estimated that only 4 V will be required to increase the spacing to 600 nm. An initial side pillar spacing of 40  $\mu\text{m}$  was used to support the waveguides and our SEM images showed this offered enough support to avoid the suspended waveguides from collapsing. The next step is to optimize the dimensions of the waveguide structure and to demonstrate the MEMS and optical functionality.

This work was supported by the Engineering and Physical Sciences Research Council under Grant EP/J012823/1 and EP/J012874/1. The data used in this work will be accessible at [7].

## REFERENCES

- [1] N. Yazdi, F. Ayazi, and K. Najafi, "Micromachined inertial sensors," *Proc. IEEE* 86, 1640-1658 (1998).
- [2] R. Bashir, "BioMEMS: State-of-the-art in detection, opportunities and prospects," *Adv. Drug Deliv. Rev.* 56, 1565-1586 (2004).
- [3] G. M. Whitesides, "The origins and the future of microfluidics," *Nature* 442, 368-373 (2006)
- [4] D. J. Beebe, G. A. Mensing, and G. M. Walker, "Physics and application of microfluidics in biology," *Annu. Rev. Biomed. Eng.* 4, 261-286 (2002).
- [5] P. Horak, W. Stewart, and W. H. Loh, "Continuously tunable optical buffer with a dual silicon waveguide design," *Opt. Express* 19, 12456-12461 (2011).
- [6] W. H. Ng, N. Podoliak, P. Horak, J. Wu, H. Liu, W. J. Stewart, and A. J. Kenyon, "Design and fabrication of suspended indium phosphide waveguides for MEMS-actuated optical buffering," *IEEE J. Sel. Topics Quantum Electron.* 21(4), 4400107 (2015).
- [7] University of Southampton eprints, <http://eprints.soton.ac.uk/id/eprint/375764>